Design and Performance of an Ultraviolet Resonance Raman Spectrometer for Proteins and Nucleic Acids*

Malcolm P. Russell, Stanislav Vohník, and George J. Thomas, Jr.
Division of Cell Biology and Biophysics School of Biological Sciences, University of Missouri–Kansas City, Kansas City, Missouri 64110-2499 USA

ABSTRACT We describe an ultraviolet resonance Raman (UVRR) spectrometer appropriate for structural studies of biological macromolecules and their assemblies. Instrument design includes the following features: a continuous wave, intracavity doubled, ultraviolet laser source for excitation of the Raman spectrum; a rotating cell (or jet source) for presentation of the sample to the laser beam; a Cassegrain optic with f/1.0 aperture for collection of the Raman scattering; a quartz prism dispersing element for rejection of stray light and Rayleigh scattering; a 0.75-m single grating monochromator for dispersion of the Raman scattering; and a liquid-nitrogen-cooled, charge-coupled device for detection of the Raman photons. The performance of this instrument, assessed on the basis of the observed signal-to-noise ratios, the apparent resolution of closely spaced spectral bands, and the wide spectrometer bandpass of 2200 cm^{-1}, is believed superior to previously described UVRR spectrometers of similar design. Performance characteristics of the instrument are demonstrated in UVRR spectra obtained from standard solvents, *p*-ethylphenol, which serves as a model for the tyrosine side chain, the DNA nucleotide deoxyguanosine-5′-monophosphate, and the human tumor necrosis factor binding protein, which is considered representative of soluble globular proteins.

INTRODUCTION

Ultraviolet resonance Raman (UVRR) spectroscopy provides a unique and versatile probe of molecular structure and dynamics. In recent years, applications in structural biology have increased greatly in both scope and number. With appropriate selection of the wavelength of excitation of the UVRR spectrum, it is possible to acquire biomolecular vibrational information not obtainable either by conventional off-resonance Raman spectroscopy or by alternative spectroscopic approaches. Information so obtained can be useful in the diagnosis of structures, interactions, and macromolecular environments of aromatic amino acids in proteins and of purine and pyrimidine bases in nucleic acids. Comprehensive reviews have been given by Austin et al. (1993) and Thomas and Tsuboi (1993).

One indication of the increasing use of the UVRR method in structural biology is the large number of recent reports describing UV laser Raman instrumentation for biological applications. In the majority of cases, a pulsed laser has been employed as the Raman excitation source (Su et al., 1990; Teraoka et al., 1990; Kaminaka and Kitagawa, 1992; Asher, 1993; Hashimoto et al., 1993; Manoharan et al., 1993; Toyama et al., 1993; Leonard et al., 1994; Tomkova et al., 1994). However, use of the pulsed laser is plagued with the fundamental problem of Raman saturation, i.e., the depopulation of the ground electronic state and overpopulation of an excited electronic state (Johnson et al., 1986). Such population inversion in the target molecules can lead to severe attenuation of the Raman band intensities. Accordingly, the power of the laser pulse must be kept low, a situation not conducive to achieving good spectral quality. A more favorable UVRR excitation source is the continuous wave (CW) laser, since it may be implemented with power levels sufficiently low to reduce the likelihood of population inversion, yet sufficiently high to yield spectra of acceptable signal-to-noise quality. Another important consideration in UVRR spectrometer design is the rejection of visible and ultraviolet stray light, which can otherwise overwhelm the detector and obscure the UVRR spectrum. While multiple grating spectrometers offer superior stray light rejection, the percentage of Raman scattered light reaching the detector (throughput) diminishes greatly with each dispersing element. For example, the throughput of a widely used commercial triple monochromator system has been estimated as 7% at best (Asher, 1993). A triple monochromator is therefore ill suited to measuring the intrinsically feeble Raman scattering spectra typical of biological samples. On the other hand, while the single monochromator offers the greatest throughput, it is disadvantaged by low efficiency in stray light rejection. In many laboratories, the double grating monochromator system has been selected to achieve a reasonable compromise between stray light rejection and Raman throughput. Recently, Hashimoto and co-workers have also demonstrated that an instrument combining a single grating monochromator with a more efficient premonochromator dispersing element, such as the quartz prism, can provide both satisfactory stray light rejection and sufficient throughput for UVRR spectroscopy (Hashimoto et al., 1993).

It is usually convenient and sometimes necessary in biological applications to compare the intensities of Raman bands which are greatly separated in wavenumber value

Received for publication 26 October 1994 and in final form 20 January 1995.

Address reprint requests to George J. Thomas, Jr., Division of Cell Biology and Biophysics, School of Biological Sciences, University of Missouri-Kansas City, Kansas City, MO 64110-2499. Tel.: 816-235-5247; Fax: 816-235-5158; E-mail: thomasgj@vax1.umkc.edu.

This is Paper 47 in the series "Structural Studies of Viruses by Raman Spectroscopy."

© 1995 by the Biophysical Society

0006-3495/95/04/1607/06 $2.00

(Tuma et al., 1993). For example, in UVRR spectra of proteins, the aromatic amino acid residues exhibit resonance enhanced vibrational bands in both the regions 500–1100 cm^{-1} and 1100–1700 cm^{-1}. Also, in metalloproteins, Raman bands which are in the region below 500 cm^{-1} (metal-ligand stretching modes) and in the region above 2000 cm^{-1} (CO or CN stretching modes) may be of simultaneous interest. The capability of a spectrometer system to achieve an effective bandpass as large as 2000 cm^{-1} is of importance in such applications. In previously described UVRR instruments, the bandpass is typically less than 1000 cm^{-1}. Larger spectral ranges can be displayed only by piecing together separately recorded segments of the spectrum, a procedure which complicates the comparison of band intensities and consumes both time and material. In this paper we report the design of a UVRR spectrometer system which simultaneously achieves exceptional stray light rejection, high Raman sensitivity, and a wide spectral bandpass suitable for biological applications. These performance characteristics are accomplished with the combined use of an intracavity frequency-doubled CW laser, quartz prism predisperser, single monochromator, and CCD detector. The high quality of UVRR data collected on this instrument is exemplified for both protein and nucleic acid model compounds. Comparison of the presently obtained UVRR spectra with those reported previously demonstrates clear-cut performance advantages of this spectrometer system.

INSTRUMENTATION

The laser, monochromator, detector, and optical components of the ultraviolet resonance Raman (UVRR) instrument are illustrated in Figs. 1 and 2. In the configuration shown, the liquid sample is contained in a spinning quartz cell for presentation to the exciting radiation, which is directed toward the cell along the laboratory Z axis. Alternatively, the sample may be presented as a microjet. In either case, the Raman scattering is collected at 90°, i.e., along the laboratory Y axis. The CW ultraviolet source is a frequency doubled argon laser, Innova model 300 FRED (Coherent, Inc., Santa Clara, CA). The laser employs a thermostatted and interchangeable β-barium borate (BBO) crystal to achieve intracavity doubling of the selected argon emission line. The available UV laser emission wavelengths (and corresponding output powers in milliwatts) are 264 (20), 257 (100), 248 (30), 244 (100), 238 (30), and 229 nm (10 mW) (Asher et al., 1993). As shown in Fig. 1, the laser is directed toward the sample by means of UV-protected aluminum mirrors, M1 and M2 (Newport, Irvine, CA), and a fused silica F/4 lens, L1 (Ealing Electrooptics, Holliston, MA). Rotation of the cell is accomplished with a custom designed precision assembly, consisting of a 3000-rpm motor and fabricated axial connector. The 90° Raman scattering is gathered efficiently by the F/1 Cassegrain quartz collection optics (Applied Photophysics Ltd., London, UK) and focused by quartz lens L2 onto the entrance slit of the prism predisperser, model 608, M1 (McPherson Instruments, Acton, MA). For optional measurement of Raman depolarization ratios, the quartz polarization analyzer (A) and scrambler (S) (Karl Lambrecht, Chicago, IL) may be inserted between L2 and the predisperser. After this initial (premonochromator) dispersion stage, the scattered beam enters the single grating 0.75-m F/6 monochromator, model 750 M (SPEX Ind., Edison, NJ). The monochromator is fitted with a 2400 groove/mm holographic ruled grating blazed at 400 nm. The fully dispersed beam is then directed to a liquid-nitrogen-cooled, UV-coated, CCD detector of 1024 × 256 pixels, model 1024 × 256–2 (SPEX Ind.). Data collection and manipulation are performed on a microcomputer (Intel 486 processor) using DM3000 software (SPEX Ind.). UVRR spectra were collected with the mechanical slit widths of the premonochromator and monochromator set at 60 μm and 2 mm, respectively, yielding an effective spectral resolution of approximately 5 cm^{-1} for 244 nm excitation. Interference from cosmic rays was eliminated from the spectra using appropriate software routines. Wavenumber calibration in UV-laser excited Raman spectra was performed using the well

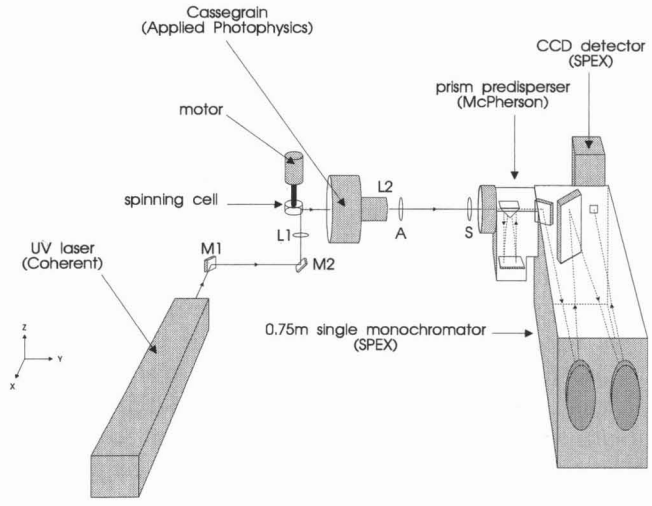

FIGURE 1 Laser, monochromator, detector, and optical components of the ultraviolet resonance Raman spectrometer system. The indicated components, as well as the spinning sample cell assembly, are mounted on a vibration-damped optical bench (laboratory XY-plane). The laser emission, initially along the laboratory X axis, is directed by mirrors M1 and M2 to impinge on the sample cell along Z, and the Raman scattering is collected at 90° (along Y).

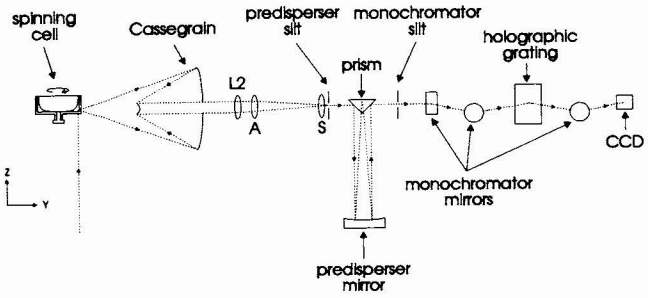

FIGURE 2 Diagram of the optical configuration in the YZ plane of the UVRR spectrometer of Fig. 1.

known Raman lines of dioxane, carbon tetrachloride, and acetonitrile (Loader, 1970). Visible excitation of off-resonance Raman spectra, for comparison with UVRR spectra, was accomplished with the argon 514.5 nm line from an Innova model 70–4 laser (Coherent, Inc.). The off-resonance Raman spectra were collected at 5 cm^{-1} resolution on a model 1877 Triplemate spectrometer (SPEX Ind.) described previously (Reilly and Thomas, 1994). Off-resonance Raman wavenumber calibration was performed with indene.

RESULTS AND DISCUSSION

UV-excited Raman spectra of acetonitrile and carbon tetrachloride

To evaluate the overall efficiency of the optical system, we obtained the UV-excited Raman spectrum of a mixture of acetonitrile and carbon tetrachloride (4:1 v/v), a sample which is expected to exhibit intense Raman bands in the UV spectral range of interest. The Raman spectrum of the CH_3CN/CCl_4 mixture, excited at 244 nm, is given in Fig. 3. The spectral trace shown in Fig. 3 represents the raw data as actually acquired, without correction for background or Rayleigh scattering and without subtraction of interference from the quartz sample cell. This spectrum, which required an accumulation time of only 60 s, exhibits a signal-to-noise (S/N) quality superior to that of previously reported spectra (Hashimoto et al., 1993). The Fig. 3 spectrum also exhibits a very low background, indicative of efficient rejection of visible stray light, and excellent discrimination against Rayleigh scattering for Raman shifts as low as 150 cm^{-1}. The Fig. 3 spectral band pass of ~2200 cm^{-1} is considerably greater than has been achieved with other recently described UVRR instrumentation (Kaminaka and Kitagawa, 1992; Asher, 1993; Hashimoto et al., 1993).

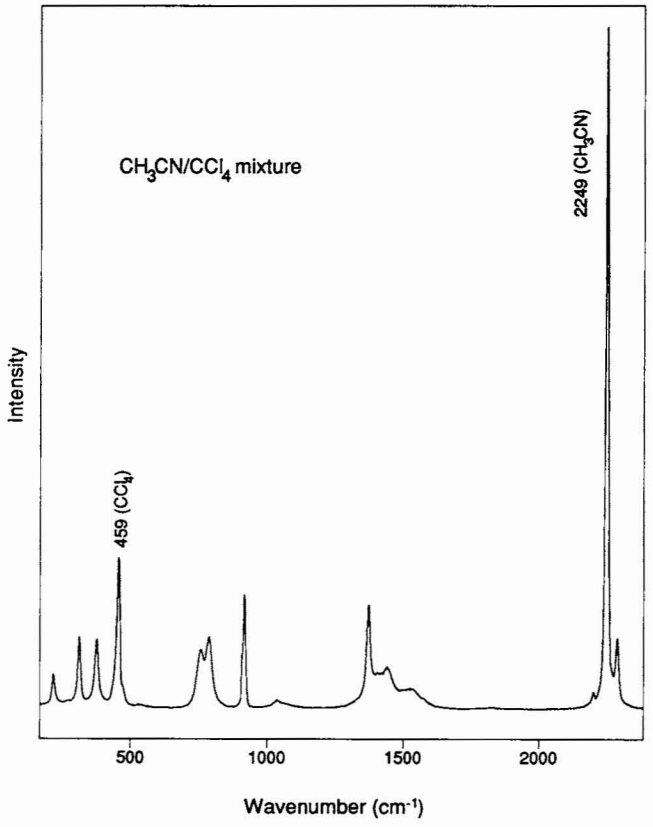

FIGURE 3 UV-excited Raman spectrum (150–2350 cm^{-1}) of a mixture of acetonitrile and carbon tetrachloride (4:1 v/v). Excitation wavelength = 244 nm; laser power at the sample = 3 mW; data acquisition time = 60 s. Labels indicate frequencies in cm^{-1} of representative Raman bands of CH_3CN and CCl_4. Because of the very intense Raman scattering of the liquid sample, no interfering Raman bands of quartz are apparent in this spectrum, and therefore no quartz correction has been applied (compare with Fig. 5).

UVRR spectrum of the tyrosine model compound *p*-ethylphenol

A cyclohexane solution of *p*-ethylphenol (PEP) is of interest to demonstrate the performance of the UVRR instrument. PEP serves both as an analogue of the tyrosine side chain in proteins and as a phenolic model compound which is expected to exhibit a Fermi doublet in the 820–850 cm^{-1} interval diagnostic of parahydroxyl hydrogen bonding (Siamwiza et al., 1975; Overman et al., 1994). The wavelength maxima of $B_{a,b}$, L_a, and L_b electronic bands are very similar in absorption spectra of PEP (198, 224, and 282 nm; M. P. Russell and G. J. Thomas, Jr., unpublished observations) and tyrosine (193, 223, and 275 nm; Fodor et al., 1989).

Fig. 4 compares the 244 nm UVRR spectrum (*bottom*) and the 514.5 nm off-resonance Raman spectrum (*top*) of PEP in cyclohexane solution. The quality of the UVRR spectrum is remarkably high, exhibiting S/N comparable to that of the off-resonance spectrum. Many of the solute bands, including the Fermi doublet components at 820 and 838 cm^{-1}, are labeled in Fig. 4. Interestingly, the estimated Fermi doublet intensity ratio, measured as the quotient of peak heights (I_{838}/I_{820} = 2.3), is virtually invariant to the change of excitation wavelength from 514.5 to 244 nm. On the other hand, dramatic resonance enhancement is observed for PEP Raman bands at 1173, 1614, and 1660 cm^{-1}, while modest enhancement is evident for bands at 642 and 1204 cm^{-1}. Excitation of phenol derivatives at wavelengths below 244 nm has been shown previously to affect many tyrosine band intensities including the Fermi doublet intensity ratio (Fodor et al., 1989).

Using the solvent band at 1444 cm^{-1} as an intensity reference, Fig. 4 indicates an approximate sevenfold resonance enhancement of the 1614 cm^{-1} band of PEP and an even greater relative enhancement for the 1660 cm^{-1} band. The data of Fig. 4 are the first to demonstrate a resonance enhanced mode of the paraphenolic residue at 1660 cm^{-1}. Spectra collected from more dilute PEP solutions at exposure times as short as 2 s (data not shown), as well as previously reported UVRR spectra (Johnson et al., 1986), confirm that the 1660 cm^{-1} band is not the result of sample photodecomposition. Probable assignments are to an overtone ($2 \times \sigma_{10a}$) or combination mode ($\sigma_{18a} + \sigma_{6b}$), in accordance with previously reported vibrational spectra of *p*-cresol (Takeuchi

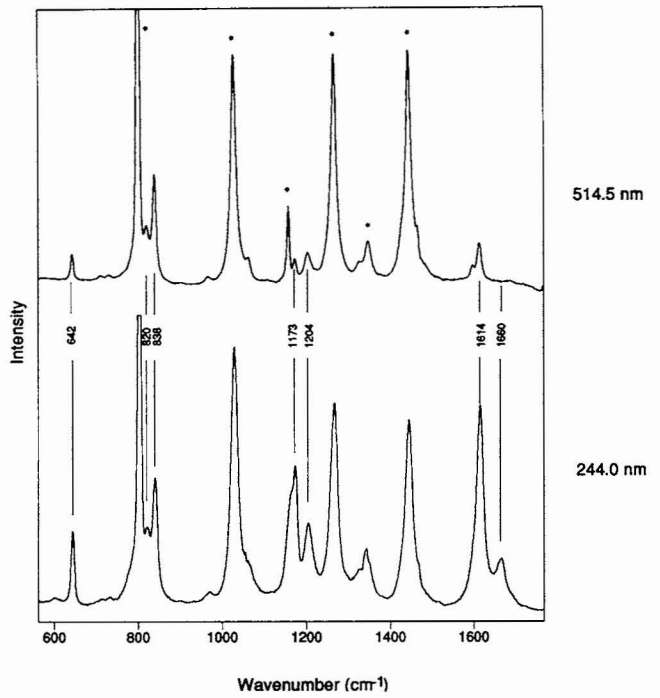

FIGURE 4 Raman spectra (550–1750 cm^{-1}) of solutions of PEP in cyclohexane. The UVRR spectrum (*bottom*) was obtained from 0.3 M PEP excited at 244 nm (3 mW), and the off-resonance spectrum (*top*) from 1.0 M PEP excited at 514.5 nm (200 mW). Data acquisition time = 10 min. Frequencies of prominent Raman bands of PEP are labeled in cm^{-1} units. Asterisks identify prominent bands of the cyclohexane solvent. These exhibit slight dependence of intensity upon excitation wavelength, suggesting probable preresonance enhancement at 244 nm.

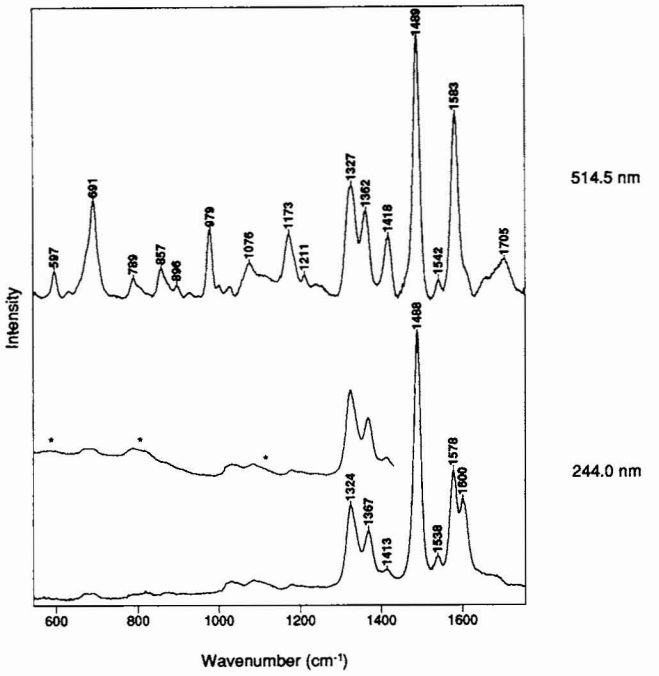

FIGURE 5 Raman spectra (550–1750 cm^{-1}) of solutions of 5′-dGMP in H_2O. The UVRR spectrum (*bottom*) was obtained from 2 mM 5′-dGMP excited at 244 nm (2 mW) and was corrected for the weak bands of quartz below 1100 cm^{-1} (indicated by asterisks in the middle trace). (Quartz contributes no bands above 1100 cm^{-1}.) The off-resonance spectrum (*top*) was obtained from 250 mM 5′-dGMP excited at 514.5 nm (200 mW). Data acquisition time = 10 min. Frequencies of prominent Raman bands of 5′-dGMP are labeled in cm^{-1} units.

et al., 1988). The presently employed UV excitation wavelength of 244 nm lies closer to the L_a (224 nm) than to the L_b (282 nm) absorption band of PEP. Accordingly, it is expected that the UVRR spectrum of Fig. 4 reflects resonance enhancement primarily from the L_a absorption band. This is consistent with data on tyrosine showing that excitation within the L_a band enhances specifically the vibronically active modes σ_{9a} (1180 cm^{-1}), σ_{8b} (1601 cm^{-1}) and σ_{8a} (1617 cm^{-1}) (Fodor et al., 1989).

UVRR spectrum of a DNA nucleotide, deoxyguanosine-5′-monophosphate

Fig. 5 compares the UVRR spectrum of the DNA nucleotide deoxyguanosine-5′-monophosphate (5′-dGMP) excited at 244 nm with the off-resonance spectrum excited at 514.5 nm. Resonance enhancement is most significant for bands of 5′-dGMP above 1300 cm^{-1}, assignable to in-plane vibrations of the purine ring (Lord and Thomas, 1967; Toyama et al., 1993). The present UVRR spectrum, though obtained in only 10 min from a 2 mM solution of 5′-dGMP, exhibits improved signal intensities and resolution in comparison to those for a spectrum obtained previously on a significantly more concentrated (5 mM) solution of the nucleotide (Fodor et al., 1985). A UVRR spectrum of 1 mM 5′-dGMP excited at 260 nm has also been reported recently (Toyama et al., 1993), but does not exhibit the sharp resolution of bands at 1578 and 1601 cm^{-1} that is evident in the Fig. 5 spectrum.

The data of Fig. 5 identify several Raman bands of the guanine residue which undergo significant resonance enhancement. Table 1 lists the Raman bands exhibiting the largest enhancements, together with tentative assignments based upon the present and previous results (Lord and Thomas, 1967; Lane and Thomas, 1979; Fodor et al., 1985; Toyama et al., 1993).

UVRR spectrum of a protein: the human tumor necrosis factor binding protein

The off-resonance (514.5 nm) and UVRR spectra (244 nm) of the human tumor necrosis factor binding protein (TNFbp)

TABLE 1 Frequencies and assignments of Raman bands of 5′-dGMP exhibiting UV-resonance enhancement

Band (cm^{-1})	Assignment	Reference*
1601	Pyrimidine ring mode (and/or NH_2 scissor)	a, b, c
1578	Pyrimidine ring mode	a, b, d
1539	Imidazole ring and C6 moiety	d
1488	Imidazole ring involving the N7 moiety	c, d
1413	Imidazole ring coupled with furanose C1′ moiety	d
1367	C2=N3—C4=C5—N7=C8 stretching mode	b, c
1324	Imidazole ring coupled with C8-N9 stretch	b, c

*a, Lord and Thomas, 1967; b, Lane and Thomas, 1979; c, Fodor et al., 1985; d, Toyama et al., 1993.

are compared in Fig. 6. TNFbp was the gift of Dr. Claire L. Careaga, Synergen Inc., Boulder, CO. This unusual globular protein contains 12 cystine disulfide bonds which generate in the off-resonance spectrum an intense and complex S-S stretching band centered near 509 cm^{-1}, as well as an intense C-S stretching band near 656 cm^{-1}. [Further discussion of the off-resonance spectrum of TNFbp will be given elsewhere (Tuma, R., M. Russell, M. Rosendahl, and G. J. Thomas, Jr., manuscript in preparation).

As shown in the UVRR spectrum of TNFbp excited at 244 nm (Fig. 6, *bottom*), all of the prominent peaks can be assigned to aromatic amino acid side chains. Resonance enhancement is strong for the single tryptophan residue and five tyrosine residues per subunit, weak for the five phenylalanines, and not apparent for other residues. In particular, the disulfide related modes of cystine residues, which appear prominently with 514.5 nm excitation, are not observed in the UVRR spectrum. Fig. 6 illustrates the advantage of a wide UVRR spectrometer bandpass for visualizing relative enhancement intensities of bands distributed throughout the 500–1700 cm^{-1} interval. The high signal-to-noise quality and spectral resolution of the present UVRR spectrometer are evident in the protein UVRR spectrum of Fig. 6. These data can be compared with other recently reported UVRR spectra of soluble globular proteins (Kaminaka and Kitagawa, 1992; Hildebrandt et al., 1988).

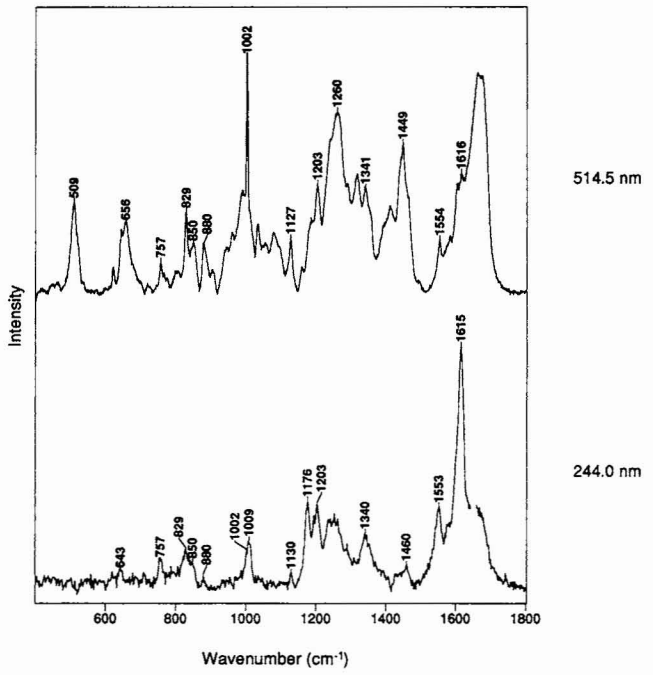

FIGURE 6 Raman spectra (400–1800 cm^{-1}) of solutions of TNFbp. The UVRR spectrum (*bottom*) was obtained from 5 mg/ml TNFbp excited at 244.0 nm (1 mW), and was corrected for bands of quartz as indicated in Fig. 5. The off-resonance spectrum (*top*) was obtained from 153 mg/ml TNFbp excited at 514.5 nm (200 mW). Data acquisition time = 60 min. Frequencies of the prominent Raman bands of TNFbp are labeled in cm^{-1} units. The amino acid sequence of the 162 residue protein is: MDSVCPQGKY IHPQNNSICC TKCHKGTYLY NDCPGPGQDT DCRECESGSF TASENHLRHC LSCSKCRKEM GQVEISSCTV DRDTVCGCRK NQYRHYWSEN LFQCFCCSLC LNGTVHLSCQ EKQNTVCTCH AGFFLRENEC VSCSNCKKSL ECTKLCLPQI EN.

Photochemical integrity of UV-irradiated samples

Continuous wave UV laser excitation sources are generally recognized as more favorable than pulsed UV laser sources for averting possible photochemical damage of biological samples (Austin et al., 1993). Indeed, for the present applications no evidence of photochemical damage was detected. In protocols employed to obtain the data of Figs. 3–6, the UVRR spectra were collected over time periods ranging from 1 s to 10 min and the spectra were invariant to the time of UV laser irradiation. Absence of photochemical damage was confirmed independently for nucleotide samples by measurement of UV absorption spectra. The UV absorption signatures were identical before and after laser irradiation.

SUMMARY AND CONCLUSIONS

We have described the design of a simple and efficient spectrometer system for application of ultraviolet resonance Raman spectroscopy to aqueous solutions of proteins and nucleic acids. Performance of the system has been demonstrated in representative applications to nucleotide and protein solutions. The present spectrometer combines several features described previously for UVRR applications, including continuous-wave UV-laser excitation (Asher et al., 1993), effective rejection of elastic scattering and stray light through tandem configuration of dispersive elements (Kaminaka and Kitagawa, 1992; Hashimoto et al., 1993), and exploitation of the efficient light gathering capability of Cassegrain optics of low f number (Kaminaka and Kitagawa, 1992). These features, together with a state-of-the-art CCD detector, provide a modular UVRR instrument of superior performance.

The UVRR spectrometer of Fig. 1 offers the following principal advantages over previously described instrumentation: 1) significant improvement in signal-to-noise ratio; 2) simultaneous improvement in spectral band resolution; 3) access to a wide interval (>2000 cm^{-1}) of the Raman vibrational spectrum, which provides for economies in time of data acquisition and quantity of biological samples; and 4) improved sensitivity for detection of Raman bands of low intensity without deleterious depopulation of the molecular electronic ground state.

The present instrumentation (Fig. 1) and sample illumination scheme (Fig. 2) permit UVRR data collections of high quality on nucleic acid analogues (Fig. 5) and proteins (Fig. 6) without compromising structural integrity of the target biomolecules. Accordingly, the methods illustrated here should permit implementation of UVRR as a probe of biologically important structural transformations of nucleic acids, proteins, and their assemblies. Preliminary results obtained in our laboratory indicate that the present instrumentation will be useful in studies of structural polymorphism of nucleic acids, conformational transitions affecting protein side-chain environments, and mechanisms of virus assembly.

We thank Prof. Hideo Takeuchi and Dr. Takashi Miura (Tohoku University, Sendai, Japan) for advice and assistance, Prof. Teizo Kitagawa (Institute for Molecular Science, Okazaki, Japan) for providing access to results in advance of publication, and Dr. Clare L. Careaga (Synergen, Inc., Boulder, CO) for the gift of human tumor necrosis factor binding protein. We also thank Prof. Ronald E. Hester and Mr. Reuben Girling (York University, UK) for contributing to the design of the spinning sample cell used in this work. This work was supported by grants GM50776 and AI18758 from the National Institutes of Health.

REFERENCES

Asher, S. A. 1993. UV resonance Raman spectroscopy for analytical, physical, and biophysical chemistry: Part 1. *Anal. Chem.* 65:59A–66A.

Asher, S. A., R. W. Bormett, X. G. Chen, D. H. Lemmon, N. Cho, P. Peterson, M. Arrigoni, L. Spinelli, and J. Cannon. 1993. UV resonance Raman spectroscopy using a new cw laser source: convenience and experimental simplicity. *Appl. Spectrosc.* 47:628- 633.

Austin, J. C., T. Jordan, and T. G. Spiro. 1993. Ultraviolet resonance Raman studies of proteins and related model compounds. *In* Advances in Spectroscopy, Vol. 20A. R. J. Clark and R. E. Hester, editors. John Wiley & Sons, London.

Fodor, S. P. A., R. P. Rava, T. R. Hays, and T. G. Spiro. 1985. Ultraviolet resonance Raman spectroscopy of the nucleotides with 266-, 240-, 218-, and 200-nm pulsed laser excitation. *J. Am. Chem. Soc.* 107:1520–1529.

Fodor, S. P. A., R. A. Copeland, C. A. Grygon, and T. G. Spiro. 1989. Deep-ultraviolet Raman excitation profiles and vibronic scattering mechanisms of phenylalanine, tyrosine and tryptophan. *J. Am. Chem. Soc.* 111:5509–5518.

Hashimoto, S., T. Ikeda, H. Takeuchi, and I. Harada. 1993. Utilization of a prism monochromator as a sharp-cut bandpass filter in ultraviolet Raman spectroscopy. *Appl. Spectrosc.* 47:1283–1285.

Hildebrandt, P. G., R. A. Copeland, T. G. Spiro, J. Otlewski, M. Laskowski, Jr., and F. G. Prendergast. 1988. Tyrosine hydrogen-bonding and environmental effects in proteins probed by ultraviolet resonance Raman spectroscopy. *Biochemistry.* 27:5426–5433.

Johnson, C. R., M. Ludwig, and S. A. Asher. 1986. Ultraviolet resonance Raman characterization of photochemical transients of phenol, tyrosine and tryptophan. *J. Am. Chem. Soc.* 108:905–912.

Kaminaka, S., and T. Kitagawa. 1992. A novel idea for practical UV resonance Raman measurement with a double monochromator and its application to protein structural studies. *Appl. Spectrosc.* 46:1804–1808.

Lane, M., and G. J. Thomas, Jr. 1979. Kinetics of hydrogen-deuterium exchange in guanosine 5′-monophosphate and guanosine 3′:5′-monophosphate determined by laser Raman spectroscopy. *Biochemistry.* 18:3839–3846.

Leonard, J. D., Jr., G. Katagiri, and T. L. Gustafson. 1994. Quasi-continuous generation of 211-nm excitation for resonance Raman spectroscopy. *Appl. Spectrosc.* 48:489–492.

Loader, J. 1970. Basic Laser Raman Spectroscopy. Heyden & Sons, Ltd., London.

Lord, R. C., and G. J. Thomas, Jr. 1967. Raman spectral studies of nucleic acids and related molecules. I. Ribonucleic acid derivatives. *Spectrochim. Acta Part A.* 23:2551–2591.

Manoharan, R., E. Ghiamati, S. Chada, W. H. Nelson, and J. F. Sperry. 1993. Effect of cultural conditions on deep UV resonance Raman spectra of bacteria. *Appl. Spectrosc.* 47:2145–2150.

Overman, S. A., K. L. Aubrey, N. S. Vispo, G. Cesareni, and G. J. Thomas, Jr. 1994. Novel tyrosine markers in Raman spectra of wild-type and mutant (Y21M and Y24M) *Ff* virions indicate unusual environments for coat protein phenoxyls. *Biochemistry.* 33:1037–1042.

Reilly, K. E., and G. J. Thomas, Jr. 1994. Hydrogen exchange dynamics of the P22 virion determined by time-resolved Raman spectroscopy: effects of chromosome packaging on the kinetics of nucleotide exchanges. *J. Mol. Biol.* 241:68–82.

Siamwiza, M. N., R. C. Lord, M. C. Chen, T. Takamatsu, I. Harada, H. Matsuura, and T. Shimanouchi. 1975. Interpretation of the doublet at 850 and 830 cm^{-1} in the Raman spectra of tyrosyl residues in proteins and certain model compounds. *Biochemistry.* 14:4870–4876.

Su, C., Y. Wang, and T. G. Spiro. 1990. Saturation effects on ultraviolet resonance Raman intensities: excimer/YAG laser comparison and aromatic amino acid cross-sections. *J. Raman Spectrosc.* 21:435–440.

Takeuchi, H., N. Watanabe, and I. Harada. 1988. Vibrational spectra and normal coordinate analysis of *p*-cresol and its deuterated analogs. *Spectrochim. Acta Part A.* 44:749–761.

Teraoka, J., P. A. Harmon, and S. A. Asher. 1990. UV resonance Raman saturation spectroscopy of tryptophan derivatives: photophysical relaxation measurements with vibrational band resolution. *J. Am. Chem. Soc.* 112:2892–2900.

Thomas, G. J., Jr., and M. Tsuboi. 1993. Raman spectroscopy of nucleic acids and their complexes. *In* Advances in Biophysical Chemistry, Vol. 3. C. A. Bush, editor. JAI Press, Inc., Greenwich, CT.

Tomkova, A., L. Chinsky, P. Miskovsky, P., and P. Y. Turpin. 1994. A-Z conformational transition in poly(rA-rU) and structure marker bands in UV resonance Raman spectroscopy. *J. Mol. Struct.* 318:65–77.

Toyama, A., Y. Takino, H. Takeuchi, and I. Harada. 1993. Ultraviolet resonance Raman spectra of ribosyl C(1′)-deuterated purine nucleosides: evidence of vibrational coupling between purine and ribose rings. *J. Am. Chem. Soc.* 115:11092–11098.

Tuma, R., S. Vohník, H. Li, and G. J. Thomas, Jr. 1993. Cysteine conformation and sulfhydryl interactions in proteins and viruses. 3. Quantitative measurement of Raman S-H band intensity and frequency. *Biophys. J.* 65:1066–1072.